

## Low dose-rate irradiation with [<sup>3</sup>H]-labelled valine to selectively target hypoxic cells in a human colorectal cancer xenograft model

Stine Gyland Mikalsen, Lars Tore Gyland Mikalsen, Joe Alexander Sandvik, Eva-Katrine Aarnes, Siri Fenne, Kjersti Flatmark, Heidi Lyng, Nina Frederike Jeppesen Edin & Erik Olai Pettersen

To cite this article: Stine Gyland Mikalsen, Lars Tore Gyland Mikalsen, Joe Alexander Sandvik, Eva-Katrine Aarnes, Siri Fenne, Kjersti Flatmark, Heidi Lyng, Nina Frederike Jeppesen Edin & Erik Olai Pettersen (2018) Low dose-rate irradiation with [<sup>3</sup>H]-labelled valine to selectively target hypoxic cells in a human colorectal cancer xenograft model, Acta Oncologica, 57:9, 1216-1224, DOI: [10.1080/0284186X.2018.1457223](https://doi.org/10.1080/0284186X.2018.1457223)

To link to this article: <https://doi.org/10.1080/0284186X.2018.1457223>

 View supplementary material 

 Published online: 09 Apr 2018.

 Submit your article to this journal 

 Article views: 909

 View related articles 

 View Crossmark data 

ORIGINAL ARTICLE



## Low dose-rate irradiation with [<sup>3</sup>H]-labelled valine to selectively target hypoxic cells in a human colorectal cancer xenograft model

Stine Gyland Mikalsen<sup>a,b</sup> , Lars Tore Gyland Mikalsen<sup>c</sup>, Joe Alexander Sandvik<sup>a</sup>, Eva-Katrine Aarnes<sup>d</sup>, Siri Fenne<sup>a</sup>, Kjersti Flatmark<sup>e</sup> , Heidi Lyng<sup>d</sup>, Nina Frederike Jeppesen Edin<sup>a</sup> and Erik Olai Pettersen<sup>a</sup>

<sup>a</sup>Department of Physics, University of Oslo, Oslo, Norway; <sup>b</sup>Department of Medical Physics, Oslo University Hospital, Oslo, Norway; <sup>c</sup>Department of Diagnostic Physics, Oslo University Hospital, Oslo, Norway; <sup>d</sup>Department of Radiation Biology, Oslo University Hospital, Oslo, Norway; <sup>e</sup>Department of Tumour Biology, Oslo University Hospital, Oslo, Norway

### ABSTRACT

**Background:** Earlier *in vitro* studies show that irradiation with an ultra-low dose-rate of 15 mGy/h delivered with [<sup>3</sup>H]-valine leads to loss of clonogenicity in hypoxic T-47D cells. Here, the aim was to determine if [<sup>3</sup>H]-valine could be used to deliver low dose-rate irradiation in a colorectal cancer model.

**Methods:** Clonogenicity was measured in cultured cancer cell line HT29 irradiated with 15 mGy/h combined with intermittent hypoxia. Mice with HT29 xenografts were irradiated by repeated injections of [<sup>3</sup>H]-valine intravenously. The activity in the tumor tissue was measured by scintillation counting and tumor growth, hypoxic fraction and tritium distribution within tumors were assessed by pimonidazole staining and autoradiography.

**Results:** Ultra-low dose-rate irradiation decreased clonogenicity in hypoxic colorectal cancer cells. *In vivo*, the tumor growth, hypoxic fraction and weight of the mice were similar between the treated and untreated group. Autoradiography showed no [<sup>3</sup>H]-valine uptake in hypoxic tumor regions in contrast to aerobic tissue.

**Conclusion:** Continuous low-dose-rate irradiation was well tolerated by aerobic tissue. This indicates a potential use of low dose-rate irradiation to target hypoxic tumor cells in combination with high dose-rate irradiation to eradicate the well oxygenated tumor regions. However, [<sup>3</sup>H]-valine is not the appropriate method to deliver ultra-low dose-rate irradiation *in vivo*.

### ARTICLE HISTORY

Received 8 January 2018  
Accepted 18 March 2018

### Introduction

Tumor hypoxia is a common characteristic of many solid tumors and is associated with increased radioresistance and a more aggressive disease [1–3]. Also, many chemotherapy agents need oxygen to work efficiently and target highly proliferating cells, thereby resulting in drug resistance in hypoxic regions of the tumor [4]. Strategies to overcome tumor hypoxia include radiotherapy fractionation to allow for reoxygenation [5,6] and hypoxic radiosensitisers mimicking oxygen are currently in use clinically for treatment of head and neck cancers [7]. Other strategies include hyperbaric oxygen breathing [8], dose escalation to the hypoxic regions of the tumor [9] and inhibition of small molecules selective to hypoxic areas such as CAIX, that demonstrates anti-tumor growth and anti-metastatic effect preclinically [1,10]. However, tumor hypoxia is still difficult to adequately image and hypoxia-targeted therapies have been difficult to translate from preclinical studies into clinical routine. Thus, tumor hypoxia still adversely affects clinical outcome [2,11,12].

In the present study we have investigated the potential use of ultra-low dose-rate irradiation with incorporated [<sup>3</sup>H]-labelled valine (hereafter called [<sup>3</sup>H]-valine) to selectively target hypoxic cells in a xenograft model. Extensive *in vitro*

studies on the breast cancer cell line T-47D by our group [13,14] demonstrated a dramatic effect of the treatment with ultra-low dose-rate irradiation specifically of hypoxic but not aerobic cells, with loss of clonogenicity in about 98% of the hypoxic cell population after a few weeks of irradiation. The treatment with hypoxia or ultra-low dose-rate of 15 mGy/h irradiation was well tolerated when given separately [14]. The low dose-rate treatment is therefore selectively targeting the hypoxic cells. We hypothesise that ultra-low dose-rate irradiation could potentially eradicate the hypoxic cell fraction in the tumor, and used together with conventional cancer therapy targeting the well oxygenated cells.

The ultra-low dose-rate irradiation must be delivered to the tumor continuously over several weeks. Our *in vitro* experiments suggest that [<sup>3</sup>H]-valine is well suited for continuous treatment since valine is an essential amino acid and the degree of labelling as well as the dose-rate to the nuclei could be well controlled. However, it is not clear if [<sup>3</sup>H]-valine can be used for ultra-low dose-rate irradiation in an *in vivo* model. In the present study, we aimed to assess if incorporation of [<sup>3</sup>H]-valine into protein could be used as a source of continuous low dose-rate irradiation in a xenograft model, we first assessed the *in vitro* response of the cancer cell line

HT29 to the treatment with low dose-rate irradiation and intermittent hypoxia. We then measured turnover of [<sup>3</sup>H]-valine in a xenograft model, both to tumor and serum to determine the injection rate necessary to obtain a constant dose-rate to tumor.

The effect study was done using an HT29 xenograft model to determine the efficacy of the treatment with low dose-rate irradiation, by assessing tumor growth and hypoxic fraction in a group of mice given low dose-rate treatment in comparison to an unirradiated control group. It was found that mouse xenografts of HT29 colorectal cancer cells was a suitable model, since it was well established in our facilities and tumors contained large regions of hypoxic cells. To visualise hypoxia we stained with pimonidazole, a robust and effective marker of tumor hypoxia [15]. We further calculated the dose-rate to the tumors and studied the incorporation of [<sup>3</sup>H] in detail by autoradiography to determine the distribution of irradiation within the tumors.

## Material and methods

### Cell culture

The human colorectal cancer cell line HT29 (ATCC, Manassas, VA, USA) and prostate cancer cell line PC-3 [16] were maintained in Roswell Park Memorial Institute medium (RPMI) 1640 medium supplemented with 2 mM glutamax, 1 mM Hepes and 9% fetal bovine serum at 37 °C in air with 5% carbon dioxide (all the reagents from Sigma, St. Louis, MO, USA). The cell lines were free from mycoplasma infection and cell line identity was validated by short tandem repeat analysis.

### Flow cytometry

DNA analysis of cell nuclei was performed by adapting the method from Vindelov et al. [17] as described previously [18]. Briefly, cells were prepared into a single-cell suspension, washed in 0.9% sodium chloride (NaCl) before citrate buffer was added and the cells were incubated for 30 min. A trypsin-detergent solution was added for 22 min, followed by the addition of a trypsin-inhibitor for 10 min. The samples were then incubated with a propidium iodide -containing solution for 30 min and run on a BD Accuri C6 Flow cytometer (BD Biosciences, San Jose, CA, USA).

### Measurement of pericellular oxygen concentration

An Invivo2 400 hypoxia glove-box (Ruskin, Bridgend, UK) was used to control the micro-environment with reduced oxygenation, operated to contain 4% oxygen and 5% carbon dioxide in the atmosphere (gas supplied by AGA, Oslo, Norway). The culture flasks had bottle caps equipped with filters to allow gas exchange. The pericellular oxygen concentrations were measured using a Unisense Profix 3.0 programme (Unisense A/S, Aarhus, Denmark) with an OX500 Unisense micro-sensor with a diameter of 25 μm, as described previously [19]. In brief, oxygen profiles were

obtained every two hours by stepwise (100 μm apart) measurements from the top of the medium down to the bottom of the flask, where the pericellular oxygen concentration was obtained.

### Dosimetry and irradiation *in vitro*

The dosimetry was adapted from the method of Goddu et al. [20] as described previously [14]. In brief, low dose-rate irradiation was delivered by incorporation of [<sup>3</sup>H]-valine (TRK533, L-[3,4(n)-<sup>3</sup>H]-valine, 1 mCi/ml, Amersham, GE Healthcare, Buckinghamshire, UK) into cellular protein. Cells were grown in medium supplemented with 2 or 0.33 Ci/mole [<sup>3</sup>H]-valine. Median diameters of cells and nuclei were measured by image analysis using the Gnu Image Manipulation program (GIMP) 2.8 software, where the diameter was measured in phase-contrast photographs of 123 and 153 cells and nuclei, respectively, each giving a histogram showing size-distributions (Supplementary Figure 1). Median values were 16 ± 0.2 and 13.2 ± 0.2 μm and corresponding volumes were calculated using:  $V = (\frac{4}{3}) \pi r^3$ . Whole cells and nuclei were prepared for scintillation counting as described previously [13,21] and cell and nuclear activity was measured on a scintillation counter (Packard TRI-CARB2100TR, Perkin Elmer, Waltham, MA, USA).

### Measurement of the surviving fraction by clonogenic ability

The HT 29 cells were trypsinised and each treatment group (15 mGy/h, 2.5 mGy/h and control) was counted on a flow cytometer separately and diluted to 200 cells before five parallel flasks were seeded from the irradiated as well as unirradiated cell dilutions. After about 16 days of incubation in medium without [<sup>3</sup>H]-valine, the cells were fixated, stained with methylene blue and colonies >50 cells were scored.

### Animal experiments

To study turnover of [<sup>3</sup>H]-valine in the tumors, PC-3 prostate cancer cells were used in a xenograft mouse model. Tumors were generated by subcutaneous injection of one million cells in the flank of athymic nude mice (Balb NCR mice). One intravenous (i.v.) injection of 41.7 μCi [<sup>3</sup>H]-valine was given at the start of the experiment. One unirradiated control mouse and three mice given the [<sup>3</sup>H]-valine injection were sacrificed twice per week. Tumor tissue was prepared for scintillation counting to determine the dose rate to the tumor. The tumor, liver, kidney, small intestine and lung were collected and casted into paraffin blocks.

The treatment effect was studied in the HT29 colorectal cancer xenografts mouse model. Tumors were generated by subcutaneous injection of one million cells into both left and right flank of athymic nude mice (Hsd: Athymic Nude-Foxn1nu). The mice were weighed and tumor growth was monitored by caliper measurements at least three times a week. Tumor volume was calculated by using  $V = \frac{1}{2} a \times b^2$ , where  $a$  and  $b$  were the largest and smallest perpendicular

tumor diameters, respectively. The experiment was divided into two groups: control group (seven animals) and treatment group (eight animals). When the tumor volume reached approximately 200 mm<sup>3</sup> the mice were either given an i.v. injection of 41.7 μCi [<sup>3</sup>H]-valine or a saline solution (0.9% NaCl). This was repeated every fourth or fifth day throughout the experiment. After 25 days the mice were sacrificed and tumors were collected by autopsy and sliced in two. One part was prepared for scintillation counting to determine the radioactivity in the tumor and the other part was collected and cast into paraffin blocks and hematoxylin and eosin (HE) slides.

Animal experiment protocols were approved by the institutional animal care and guidelines on animal welfare of the Norwegian National Committee for Animal Experiments were followed.

### **Preparation of tumor tissue for scintillation counting**

The tumor tissue was weighed, suspended in phosphate buffered saline (Sigma) and were turned into a cell suspension by using a mortar. The samples were centrifuged at 1400 RPM for five minutes before carefully transferring the supernatant to a scintillation tube and adding 7 millilitre of scintillation liquid for activity measurements. Two millilitre of Sodium Deoxycholate were added to the remaining tissue sample before incubation at 37 °C for 30 min. Seven millilitre of scintillation fluid were added to the samples before the activity was measured in a liquid scintillation counter. The dose-rate to the tumor was calculated by converting from activity/weight to dose/time.

### **Immunohistochemistry**

Four hours prior to euthanasia, the mice were given an injection of 80 mg/kg pimonidazole hydrochloride (1-[(2-hydroxy-3-piperidinyl)propyl]-2-nitroimidazole hydrochloride, Natural Pharmacia International Inc., Burlington, MA, USA) in 0.5 millilitre saline intraperitoneally, to label hypoxic tumor cells. Staining was assessed using primary rabbit antibody against pimonidazole (generously provided by James Raleigh, Hypoxyprobe Inc, Burlington, MA, USA) that was diluted 1:5000 with Antibody Dilution (Dako, Glostrup, Denmark). The EnVision™ method was followed (Dako). PT link (Dako) and Envision Flex target retrieval buffer (Dako) were used at pH 9 for antigen retrieval. The tissue slides were blocked with peroxidase inhibitor (H<sub>2</sub>O<sub>2</sub>), incubated with primary antibody and counterstained with hematoxylin before the slides were dehydrated and mounted.

### **Quantification of hypoxic fraction**

Consecutive sections stained with HE and pimonidazole from each tumor was imaged using one to three frames depending on size, in order to capture the whole section. In some sections minor areas were missing in the tumor periphery. The pixel size was 6.2 ± 0.1 μm. The frames of each section were merged manually to a single image. Necrotic regions

and non-tumor regions were indicated using manual delineation.

Independently, each frame was automatically segmented to identify hypoxia, as described below. They were then coregistered with the manually delineated necrosis and tumor boundaries by copying the frame positions from the manual merger. Very thin regions (62 μm) of tumor tissue located in between hypoxia and necrosis were reclassified as hypoxic tissue. Pixels identified both as hypoxic and necrotic were considered necrotic. From this, hypoxic fraction (HF), necrotic fraction (NF) and remaining tissue fractions (1-HF-NF) were computed.

Hypoxia was automatically identified through the following steps: A correction for vignetting was performed for each individual frame, using a least-square parabolic fit to the frame with all saturated (stained) pixels replaced by neighbouring values using morphological reconstruction. Following this, pixels that were dark, saturated and red were identified as pimonidazole, as described previously in [22]. Briefly, dark pixels were segmented from the blue channel of the RGB colour space. Saturation and colour were determined using the Hue-Saturation-Value colour space. The saturation channel was segmented. Red colour was determined using a fixed threshold (Hue = 0° ± 10%). Light morphological processing (radius 6.2–24.8 μm) was performed during these steps to prevent fragmentation of the hypoxic regions due to noise and granular stains.

All segmentation was performed using the algorithm by Kittler and Illingworth [23]. Manual image processing was performed using GIMP and computational image analysis using MATLAB (The MathWorks, Natick, MA, USA).

### **Autoradiography**

To assess the incorporation of radioactivity after [<sup>3</sup>H]-valine injection, autoradiographs were obtained from tissue sections of control mice (*n* = 3) and treated mice (*n* = 3). After the paraffin embedded sections were de-waxed (PT-Link (Dako)), all steps of autoradiography were carried out according to Ilford's procedures and recommendations: Nuclear Emulsion K.5 was applied directly to the de-waxed slides and stored at –20 °C for 3–4 months. After the exposure period the slides were treated with Kodak Photo-Flo 200 and developed with Ilford Phenisol and Ilford Hypam fixer. Images of the sections were taken with a Nikon D7100 camera (Nikon, New York, USA) mounted on a microscope (Nikon Diaphot, Nikon, Tokyo, Japan). The density of silver grains of each section was considered correlated to grade of incorporation of the radioactive [<sup>3</sup>H]-valine.

## **Results**

### **Dosimetry for HT29 cells**

HT29 colorectal cancer cells were irradiated with ultra-low dose-rate irradiation delivered by [<sup>3</sup>H]-valine incorporated into cellular protein. The dose-rate to the nuclei was determined by using a micro dosimetry model [20]. We measured the activity at steady-state (minimum 100 h after [<sup>3</sup>H]-valine

supplement) in whole cells and nuclei when 1.6 Ci/mole of [ $^3\text{H}$ ]-valine was added to the medium. The activity measured was  $(9.6 \pm 1.8) \times 10^{-3}$  Bq/cell and  $(4.7 \pm 0.2) \times 10^{-3}$  Bq/nucleus. The median cell and nuclei volume were determined to be  $2131 \pm 80$  and  $1222 \pm 55 \mu\text{m}^3$ , respectively. The corresponding parameter values from the model were  $S(\text{N} \leftarrow \text{N}) = 5.58 \times 10^{-4}$  Gy/Bqs and  $S(\text{N} \leftarrow \text{Cy}) = 1.30 \times 10^{-4}$  Gy/Bqs, where the  $S$ -value estimates absorbed dose rate per unit activity to the nucleus from decays either in the nucleus or cytoplasm. The dose-rate to nuclei by [ $^3\text{H}$ ]-valine irradiation was estimated to be 12 mGy/h. To achieve a dose rate of 15 mGy/h, which was used in our previous studies on T-47D breast cancer cells [13], 2 Ci/mole [ $^3\text{H}$ ]-valine was therefore added to the medium. A dose-rate of 2.5 mGy/h was achieved by 1:5 dilution of the medium containing 2 Ci/mole [ $^3\text{H}$ ]-valine.

### [ $^3\text{H}$ ]-valine irradiation *in vitro*

The HT29 cells were cultured in an atmosphere with 4% oxygen, resulting in a microenvironment with intermittent hypoxia where oxygen concentrations varied from about 3.5 to below 0.1% (Figure 1(A)). Immediately after each cell recultivation (shown with black stars), the oxygen concentration was about 3.5%. As the cells proliferated and the increasing

number of cells consumed more oxygen, the pericellular oxygen concentration gradually decreased over 2–3 days. At confluence, the oxygen concentration was below 0.1%. In a separate arm of the experiment, cells cultivated under these conditions were continuously irradiated with low dose-rate irradiation delivered by [ $^3\text{H}$ ]-valine, resulting in a dose-rate to the nucleus of 15 and 2.5 mGy/h. The plating efficiency of cells irradiated with 15 mGy/h gradually dropped to 27% after 27 days (Figure 1(B)). An even lower dose-rate of 2.5 mGy/h had a less pronounced effect on the clonogenic capacity, with 44% plating efficiency after 27 days. The cell cycle distribution was investigated by flow cytometry after 29 days of combined treatment with intermittent hypoxia and low dose-rate irradiation (Figure 1(C)). We observed an increase in fraction of cells in S-phase in irradiated cells. The fraction of cells in S-phase was 53 and 52% in cells irradiated with 15 and 2.5 mGy/h respectively, whereas in unirradiated control, grown under the same conditions, the fraction of cells in S-phase was 28%. There was no hypoxia-induced arrest in G1/S in irradiated or unirradiated cells (Figure 1(C)).

### [ $^3\text{H}$ ]-valine distribution and turnover *in vivo*

To determine the turnover of [ $^3\text{H}$ ]-valine in mice, we performed a pilot study where [ $^3\text{H}$ ]-valine was injected i.v. in

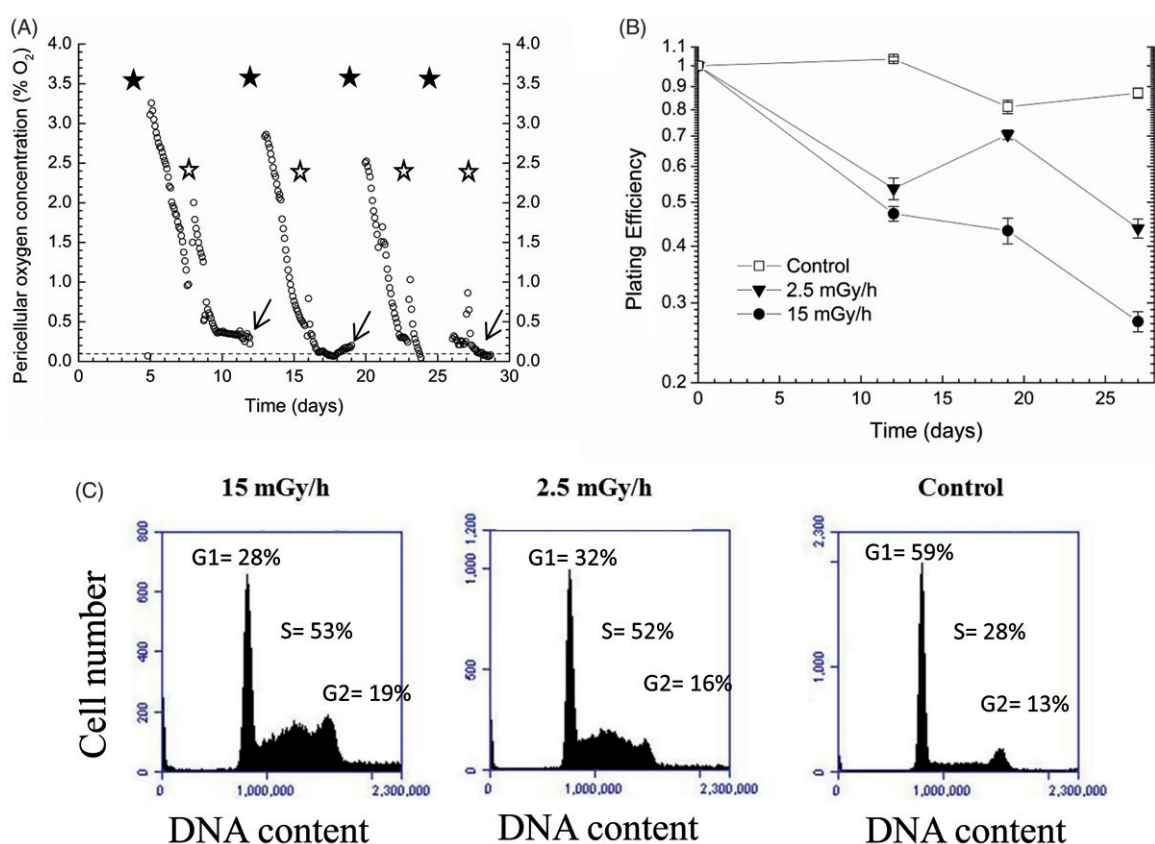


**Figure 1.** HT29 colorectal cancer cells grown in conditions of intermittent hypoxia (4% oxygen in the atmosphere) and irradiated continuously by low dose-rate [ $^3\text{H}$ ]-valine with a dose-rate of 15 or 2.5 mGy/h. Panel A shows the pericellular oxygen concentration of cells irradiated with 15 mGy/h and panel B shows the plating efficiency of cells irradiated with 15 mGy/h, 2.5 mGy/h or an unirradiated control, all seeded on the same day. At confluence, five parallel flasks were seeded for colony formation (marked with arrows in panel A). Standard errors are shown with bars. The cells were recultured four times during the experiment (black stars in panel A) and medium was changed once between recultivations (white stars). In panel C, nuclei DNA histograms of cells grown under conditions of intermittent hypoxia (4% oxygen in the atmosphere) and irradiated with 15 or 2.5 mGy/h for 29 days are shown together with an unirradiated control grown in the same conditions for 29 days.

PC-3 xenografts at the start of the experiment and the radioactivity in tumor tissue and serum was measured every 3–4 days (Figure 2). Tumor and serum activity stayed high for at least 4–5 days, with 85% of the activity left in the tumor and 74% activity left in the serum compared to one day after [<sup>3</sup>H]-valine injection, whereas after 11 days the relative activity was reduced to 19% in the tumor and 10% in the serum. To maintain a constant dose-rate to the tumor in the following effect study, [<sup>3</sup>H]-valine was injected every 4–5 days. Visual inspection of HE-slides of the tumor, liver, kidney, small intestine and lung showed no sign of tissue damage from the low dose-rate irradiation (data not shown).

### Effect of [<sup>3</sup>H]-valine treatment on tumor growth

The selective effect of low dose-rate irradiation with [<sup>3</sup>H]-valine on hypoxic cells was tested in HT29 xenografts. The mice were given i.v. injections of [<sup>3</sup>H]-valine regularly to maintain a constant dose-rate to the tumor. Tumor activity was measured to be  $75914 \pm 710$  Bq/g tumor tissue and the over-all

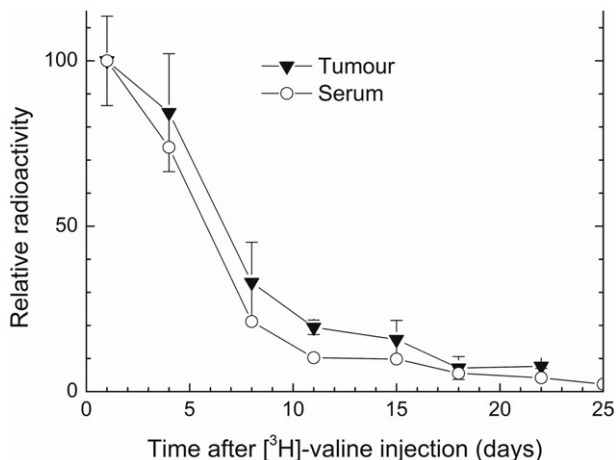


**Figure 2.** [<sup>3</sup>H]-valine turnover in tumor tissue and serum of a PC-3 prostate cancer xenograft model. Turnover of radioactivity was assessed after an initial injection of 41.7  $\mu$ Ci [<sup>3</sup>H]-valine. Every 4–5 days three mice were sacrificed and tumor activity was measured by scintillation counting. Error bars represent standard error,  $n = 3$ .

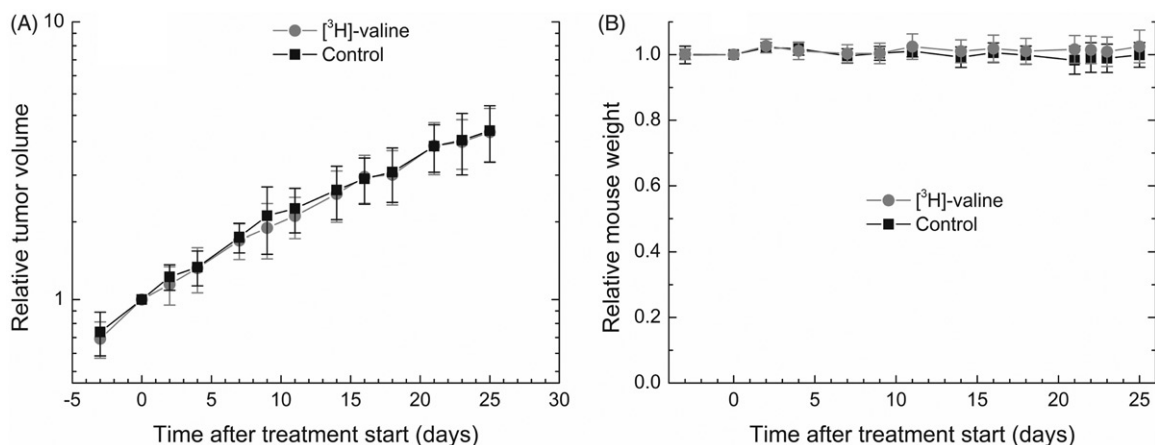


**Figure 3.** Tumor volume (panel A) and mouse weight (panel B) of HT29 colorectal cancer xenografts grown in athymic mice, that either were given continuous low dose-rate irradiation with [<sup>3</sup>H]-valine (eight mice, 16 tumors) or were untreated (control, seven mice, 14 tumors). The dose-rate was maintained constant by repeated i.v. injections of [<sup>3</sup>H]-valine. Tumor volume was measured with a caliper. Each point represents the mean of minimum 14 tumors and error bars represents standard error.

dose-rate to the tumor cells was calculated to be  $0.25 \pm 0.002$  mGy/h ( $n = 15$ ). The mean tumor growth relative to the growth at the start of treatment was similar between the low dose-rate irradiated group ( $n = 16$ ) and the control group ( $n = 14$ ) with some biological variation (Figure 3(A)). Tumor doubling time was 10.6 and 10.5 days for the irradiated and control group, respectively. The mice had no substantial weight loss throughout the experiment in either of the groups (Figure 3(B)), indicating that the treatment with ultra-low dose-rate irradiation was well tolerated.

### Hypoxia and [<sup>3</sup>H]-valine distribution within the tumor

HT29 xenografts that were not irradiated showed widespread hypoxia at tumor volumes of approximately 200 mm<sup>3</sup> (Supplementary Figure 2). Tumor hypoxia was still widespread after 25 days with continuous [<sup>3</sup>H]-valine treatment. At this time, the tumor volume was approximately 600 mm<sup>3</sup>. Large regions of necrotic tissue were observed, as showed by both HE- and pimonidazole staining of tumor sections (Figure 4(A,B)). Hypoxic regions were observed at the rim around necrotic areas, where on average (in both control and treatment group) 81% of the regions connected to necrotic areas were hypoxic. In addition, hypoxia was seen in regions not connected to necrosis. An example of the automatic segmentation of hypoxia within the tumor (red) is shown in Figure 4(C–F), together with manually delineated necrosis (yellow) and remaining viable tumor tissue (black). The mean hypoxic fraction in the [<sup>3</sup>H]-valine treated group and the control group was similar ( $0.30 \pm 0.02$  and  $0.30 \pm 0.03$ , respectively;  $p = .9$ ). The necrotic fraction was also comparable between the two groups ( $0.22 \pm 0.03$  and  $0.25 \pm 0.03$ ,  $p = .5$ ).

The distribution of incorporated radioactivity in the tumors after [<sup>3</sup>H]-valine irradiation for 25 days was determined by autoradiography on a random selection of six tumors. We compared the autoradiography slides to pimonidazole-slides from the same tumors and used neighbouring slides from the same tumor section, enabling direct comparison and recognition of the same landmarks. Hypoxia was

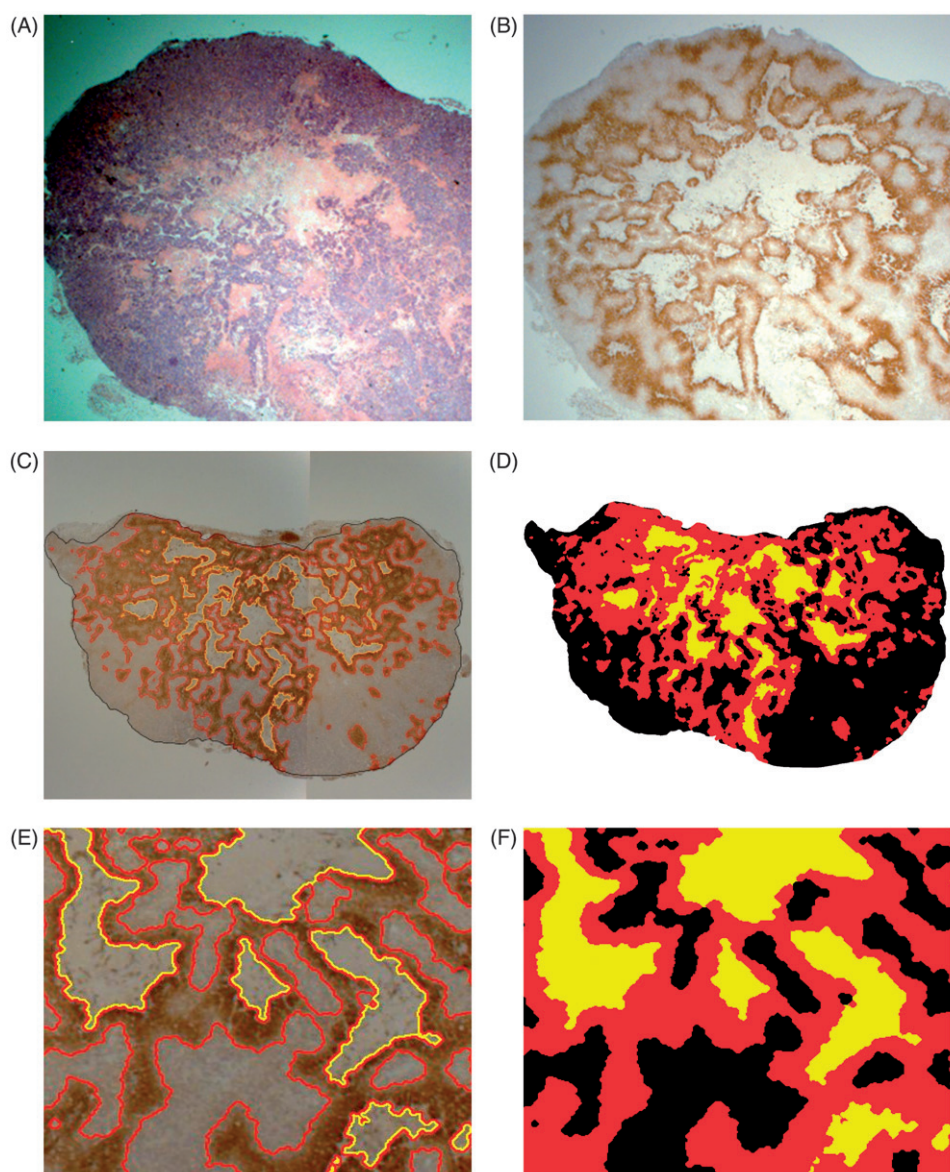


**Figure 4.** Hypoxia distribution within HT29 colorectal cancer xenografts after 25 days of treatment with ultra-low dose-rate [ $^3\text{H}$ ]-valine irradiation. The tumor volumes were approximately  $600\text{ mm}^3$ . An example is shown in panel A (HE stained slide) and panel B (pimonidazole stained slide visualizing hypoxia in brown). The tumors were widely hypoxic with areas of necrosis throughout the tumors. Hypoxic tumor regions were identified computationally and are shown in red in panels C and D, and in the excerpt in panels E and F. Necrotic regions were manually delineated by visual inspection of both pimonidazole and HE stained slides, as shown in yellow in panels C–F. The remaining tumor tissue is shown in black (panels C–F).

visualised with brown and tritium incorporation was visualised with black dots, as illustrated in an excerpt from one of the irradiated tumors in Figure 5. Hypoxic, necrotic and aerobic regions were outlined in the autoradiography slides, to determine possible overlap between these regions and [ $^3\text{H}$ ]-valine incorporation. There was no incorporation of [ $^3\text{H}$ ]-valine in necrotic areas. There was also little or no incorporation of [ $^3\text{H}$ ]-valine in hypoxic regions. In contrast, [ $^3\text{H}$ ]-valine was well incorporated in aerobic regions of the tumors (Figure 5).

## Discussion

Clonogenicity of hypoxic HT29 cells decreased after about three weeks of combined treatment with low dose-rate irradiation of  $15\text{ mGy/h}$  and intermittent hypoxia. The combined

treatment resulted in a plating efficiency of 27% in the cultured HT29 cells after 27 days of treatment (Figure 1(B)). This effect, which translates into loss of clonogenic capacity of 70% of the cell population, is probably more moderate than that observed in T-47D breast cancer cells, where 98% of the T-47D breast cancer cells lost clonogenic capacity after 3–5 weeks [13]. The oxygenation of the irradiated cells was similar in the HT29 and T-47D cell experiments; however the response may be dependent on other factors such as cell line and duration of the treatment. Several experiments with T-47D cells have been published, where a dramatic effect on surviving fraction occurred after 16–42 days. Compared to the experiments where the effect occurred after 16 days, the HT29 cells seem to be more resistant to low dose-rate irradiation than T-47D cells. However, when compared to the T-47D experiment where the effect occurred after 42 days,

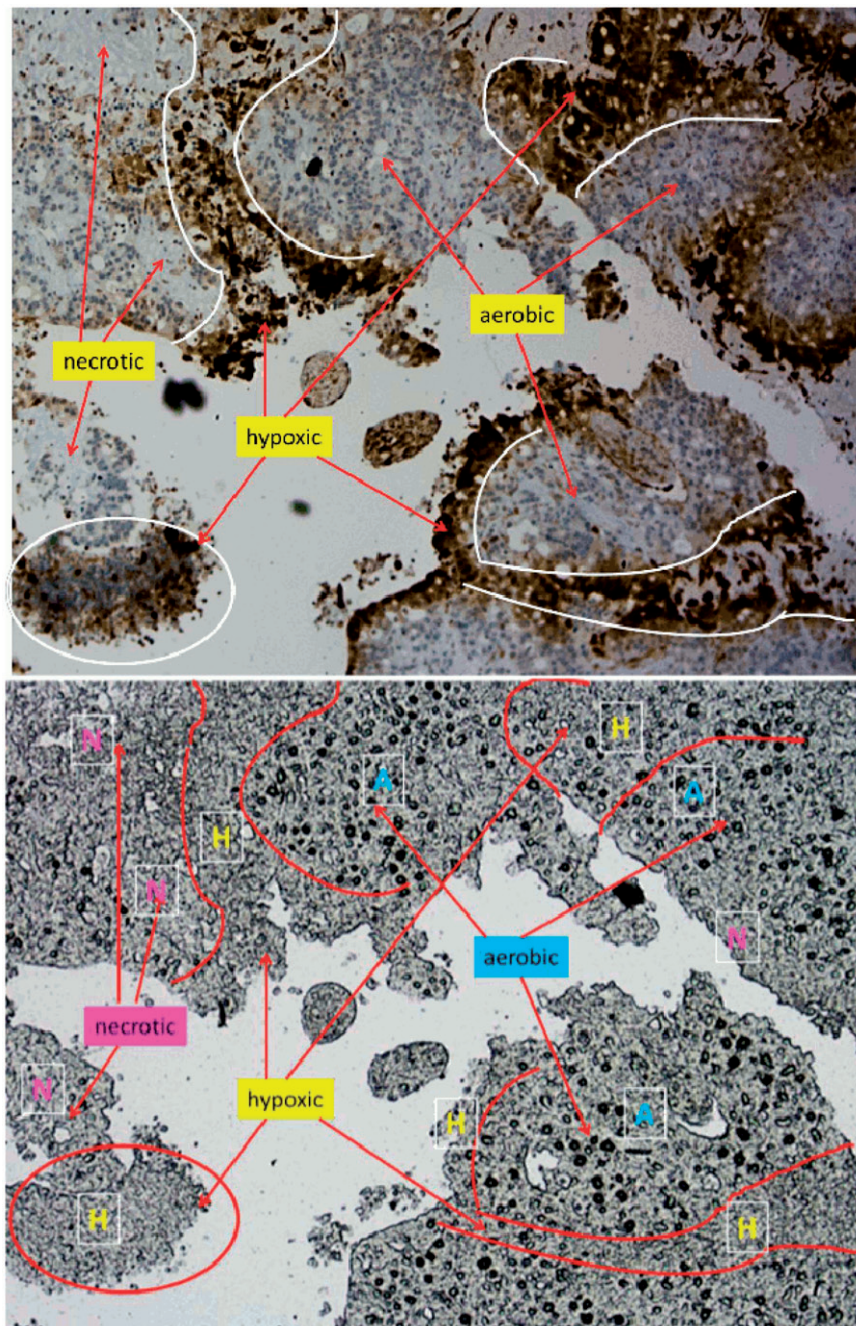


**Figure 5.** The upper panel shows an excerpt of a pimonidazole stained slide in a tumor that was given continuous low dose-rate irradiation for 25 days. The lower panel shows the same excerpt of the neighboring slide where tritium autoradiography was performed. Direct comparison between the panels was possible, since specific regions and landmarks were recognized in both panels. Aerobic (A), necrotic (N) and hypoxic (H) regions were delineated in the pimonidazole slides and transferred to the autoradiography slides, as indicated. Black spots show uptake of [ $^3\text{H}$ ]-valine, thereby visualizing [ $^3\text{H}$ ]-valine incorporation into cellular protein. There was no incorporation of [ $^3\text{H}$ ]-valine in hypoxic or necrotic regions, as shown in the lower panel. [ $^3\text{H}$ ]-valine was well incorporated in the aerobic regions.

the effect was similar with a surviving fraction of about 30% after 27 days in both cell lines. The lower dose-rate of 2.5 mGy/h resulted in a less pronounced decrease in clonogenicity, indicating that dose-rate within the range of 2.5–15 mGy/h is important for the effect. At an even higher dose-rate of 61.5 mGy/h the irradiation is no longer tolerated by aerobic T-47D cells [14].

No arrest in the hypoxia-induced checkpoint at the G1/S border was observed (Figure 1(C)). Our oxygen-sensor measures the oxygen concentration accurately down to 0.1%, but below this we can only be sure that the oxygen

concentration is lower than 0.1%. Studies on cell cycle progression under various degrees of hypoxia have shown that there is generally no inhibition of the cells in the oxygen-sensitive G1/S restriction point when the oxygen concentration is above 0.1%, while for concentrations below 0.1% oxygen, there is an increasing degree of inhibition with decreasing oxygen concentration down to 0.01% [24,25] and reviewed in [26]. S-phase accumulation, caused by slow or non-existent progression through the S-phase, is a known response to hypoxic stress [27]. Neither HT29 cells, nor T-47D breast cancer cells exposed to low dose-rate irradiation of 15 mGy/h

and intermittent hypoxia were arrested in the G1/S checkpoint [13].

The average hypoxic fraction in our study using a HT29 colorectal cancer xenograft cell model was 30%, which is comparable to what has been found previously in murine colorectal cancers (23 and 38%, respectively for HT29 and LS174T) [28,29].

In the study with [<sup>3</sup>H]-valine administrated to tumor-bearing mice, the injected tritium was incorporated into the tumor tissue, as shown by scintillation counting, but there was little, if any, uptake in hypoxic regions with viable tissue (Figure 5). This means that our model, where [<sup>3</sup>H]-valine is used to deliver ultra-low dose-rate irradiation, is not suitable to selectively target hypoxic tumor cells in a mouse model. The lack of [<sup>3</sup>H]-uptake in hypoxic tumor cells may be caused by consumption of the [<sup>3</sup>H]-valine by well oxygenated cells or by malfunctioning tumor vascularity resulting in impaired transport of [<sup>3</sup>H]-valine by blood flow to the hypoxic regions. Also, hypoxic cancer cells have a greatly reduced protein synthesis [21] and possibly also have a downregulated uptake mechanism of small molecules. This renders delivery of ultra-low dose-rate irradiation with [<sup>3</sup>H]-valine problematic. Similarly, many cytotoxic drugs will not be effectively distributed in hypoxic areas due to limited access to vessels [30,31]. Because of the low range of tritium irradiation of a maximum 6 μm [32], the treatment cannot be delivered externally. Ultra-low dose-rate irradiation might have a larger effect on intermittent hypoxic cells with another source of radiation that can be delivered externally and may therefore work better than [<sup>3</sup>H]-valine provided that the normal tissue response is limited.

When comparing the *in vitro* results on T-47D and HT29 cells with the *in vivo* results from the present effect study on HT29 xenografts, there are some aspects that need consideration. The dose-rate in the *in vitro* studies was 15 mGy/h, but was about 60 times lower in the *in vivo* studies. This would most likely result in a more moderate effect on the cell kill *in vivo*. Also, the *in vitro* experiments showed loss of clonogenicity in hypoxic cells, but no uptake of [<sup>3</sup>H]-valine was seen in hypoxic regions in the *in vivo* experiments. A marked effect on tumor growth would therefore not be expected. However, if the irradiation had reached the hypoxic regions of the tumor, we could expect a difference in the hypoxic fraction between the treated and untreated group.

In this study we investigated the effect of treatment with ultra-low dose-rate irradiation on the HT29 colorectal cancer cell line. If a suitable way to deliver the ultra-low dose-rate irradiation to the hypoxic tumor cells is found, then more cancer cell lines should be investigated in order to assess if the findings are general.

Although no treatment effect was observed *in vivo* in our study, we demonstrate that ultra-low dose-rate irradiation is well tolerated by aerobic cells in a mouse model. This has been shown previously in *in vitro* cell cultures [14] and our study demonstrates that this also is valid in an *in vivo* colorectal cancer xenograft model (Figure 3(B)), by showing that the continuous ultra-low dose-rate irradiation led to no weight loss in the mice.

## Disclosure statement

The authors report no conflict of interest.

## Funding

This work was supported by EU grant No. 222741 (METOXIA); Norges Forskningsråd (the Research Council of Norway); Kreftforeningen (the Norwegian Cancer Society) and Eckbos Legater.

## ORCID

Stine Gyland Mikalsen  <http://orcid.org/0000-0002-6476-3723>  
Kjersti Flatmark  <http://orcid.org/0000-0001-7409-0780>

## References

- [1] Pettersen EO, Ebbesen P, Gieling RG, et al. Targeting tumour hypoxia to prevent cancer metastasis. From biology, biosensing and technology to drug development: the METOXIA consortium. *J Enzyme Inhib Med Chem*. 2014;30:1–33.
- [2] Vaupel P, Mayer A. Hypoxia in cancer: significance and impact on clinical outcome. *Cancer Metastasis Rev*. 2007;26:225–239.
- [3] Vaupel P, Kallinowski F, Okunieff P. Blood flow, oxygen and nutrient supply, and metabolic microenvironment of human tumors: a review. *Cancer Res*. 1989;49:6449–6465.
- [4] Shannon AM, Bouchier-Hayes DJ, Condrón CM, et al. Tumour hypoxia, chemotherapeutic resistance and hypoxia-related therapies. *Cancer Treat Rev*. 2003;29:297–307.
- [5] Brown JM. Tumor hypoxia in cancer therapy. *Meth Enzymol*. 2007;435:297–321.
- [6] Kallman RF. The phenomenon of reoxygenation and its implications for fractionated radiotherapy. *Radiology*. 1972;105:135–142.
- [7] Bentzen J, Toustrup K, Eriksen JG, et al. Locally advanced head and neck cancer treated with accelerated radiotherapy, the hypoxic modifier nimorazole and weekly cisplatin. Results from the DAHANCA 18 phase II study. *Acta Oncol*. 2015;54:1001–1007.
- [8] Overgaard J. Sensitization of hypoxic tumour cells-clinical experience. *Int J Radiat Biol*. 1989;56:801–811.
- [9] Welz S, Monnich D, PfannenberG C, et al. Prognostic value of dynamic hypoxia PET in head and neck cancer: results from a planned interim analysis of a randomized phase II hypoxia-image guided dose escalation trial. *Radiother Oncol*. 2017;124:526–532.
- [10] Dubois L, Peeters SG, van Kuijk SJ, et al. Targeting carbonic anhydrase IX by nitroimidazole based sulfamides enhances the therapeutic effect of tumor irradiation: a new concept of dual targeting drugs. *Radiother Oncol*. 2013;108:523–528.
- [11] Hammond EM, Asselin MC, Forster D, et al. The meaning, measurement and modification of hypoxia in the laboratory and the clinic. *Clin Oncol (R Coll Radiol)*. 2014;26:277–288.
- [12] Vaupel P, Mayer A. Tumor hypoxia: causative mechanisms, micro-regional heterogeneities, and the role of tissue-based hypoxia markers. *Adv Exp Med Biol*. 2016;923:77–86.
- [13] Edin NJ, Christoffersen S, Fenne S, et al. Cell inactivation by combined low dose-rate irradiation and intermittent hypoxia. *Int J Radiat Biol*. 2015;91:336–345.
- [14] Pettersen EO, Bjorhovde I, Sovik A, et al. Response of chronic hypoxic cells to low dose-rate irradiation. *Int J Radiat Biol*. 2007;83:331–345.
- [15] Raleigh JA, Miller GG, Franko AJ, et al. Fluorescence immunohistochemical detection of hypoxic cells in spheroids and tumours. *Br J Cancer*. 1987;56:395–400.
- [16] Kaighn ME, Narayan KS, Ohnuki Y, et al. Establishment and characterization of a human prostatic carcinoma cell line (PC-3). *Invest Urol*. 1979;17:16–23.

- [17] Vindelov LL, Christensen IJ, Nissen NI. A detergent-trypsin method for the preparation of nuclei for flow cytometric DNA analysis. *Cytometry*. 1983;3:323–327.
- [18] Mikalsen SG, Jeppesen Edin N, Sandvik JA, et al. Separation of two sub-groups with different DNA content after treatment of T-47D breast cancer cells with low dose-rate irradiation and intermittent hypoxia. *Acta Radiol*. 2017;59:26–33.
- [19] Pettersen EO, Larsen LH, Ramsing NB, et al. Pericellular oxygen depletion during ordinary tissue culturing, measured with oxygen microsensors. *Cell Prolif*. 2005;38:257–267.
- [20] Goddu SM, Rao DV, Howell RW. Multicellular dosimetry for micro-metastases: dependence of self-dose versus cross-dose to cell nuclei on type and energy of radiation and subcellular distribution of radionuclides. *J Nucl Med*. 1994;35:521–530.
- [21] Pettersen EO, Juul NO, Ronning OW. Regulation of protein metabolism of human cells during and after acute hypoxia. *Cancer Res*. 1986;46:4346–4351.
- [22] Mikalsen LT, Dhakal HP, Bruland OS, et al. Quantification of angiogenesis in breast cancer by automated vessel identification in CD34 immunohistochemical sections. *Anticancer Res*. 2011;31:4053–4060.
- [23] Kittler J, Illingworth J. Minimum error thresholding. *Pattern Recognit*. 1986;19:41–47.
- [24] Bedford JS, Mitchell JB. The effect of hypoxia on the growth and radiation response of mammalian cells in culture. *Br J Radiol*. 1974;47:687–696.
- [25] Pettersen EO, Lindmo T. Inhibition of cell-cycle progression by acute treatment with various degrees of hypoxia: modifications induced by low concentrations of misonidazole present during hypoxia. *Br J Cancer*. 1983;48:809–817.
- [26] Pastorekova S, Kopacek J. Tumour hypoxia: molecular mechanisms and clinical implications. Bratislava. Frankfurt am Main: VEDA Publishing House of the Slovak Academy of Sciences; Peter Lang International Academic Publishers; 2012.
- [27] Olcina M, Lecane PS, Hammond EM. Targeting hypoxic cells through the DNA damage response. *Clin Cancer Res*. 2010;16:5624–5629.
- [28] Russell J, Carlin S, Burke SA, et al. Immunohistochemical detection of changes in tumor hypoxia. *Int J Radiat Oncol Biol Phys*. 2009;73:1177–1186.
- [29] Heijmen L, Ter Voert EG, Punt CJ, et al. Monitoring hypoxia and vasculature during bevacizumab treatment in a murine colorectal cancer model. *Contrast Media Mol Imaging*. 2014;9:237–245.
- [30] Wouters A, Pauwels B, Lardon F, et al. Review: implications of in vitro research on the effect of radiotherapy and chemotherapy under hypoxic conditions. *Oncologist*. 2007;12:690–712.
- [31] Teicher BA, Holden SA, al-Achi A, et al. Classification of antineoplastic treatments by their differential toxicity toward putative oxygenated and hypoxic tumor subpopulations in vivo in the FSaIIc murine fibrosarcoma. *Cancer Res*. 1990;50:3339–3344.
- [32] Chen J. Radiation quality of tritium. *Radiat Prot Dosimetry*. 2006;122:546–548.